Article

The Combination of Decellularized Cartilage and Amniotic Membrane Matrix Enhances the Production of Extracellular Matrix Elements in Human Chondrocytes

Antonio Rojas-Murillo [1] , Jorge Lara-Arias [2], Héctor Leija-Gutiérrez [3], Rodolfo Franco-Márquez [4] ,
Nidia Karina Moncada-Saucedo [5] , Abel Guzmán-López [6], Félix Vilchez-Cavazos [2], Elsa Nancy Garza-Treviño [1,*]
and Mario Simental-Mendía [2,*]

1 Department of Biochemistry and Molecular Medicine, Universidad Autónoma de Nuevo Leon,
  Monterrey 66460, Nuevo Leon, Mexico; juan.rojasmrll@uanl.edu.mx
2 Orthopedic Trauma Service, University Hospital "Dr. José Eleuterio González", Universidad Autónoma de
  Nuevo Leon, Monterrey 66460, Nuevo Leon, Mexico; jorge.larars@uanl.edu.mx (J.L.-A.);
  jose.vilchezcvz@uanl.edu.mx (F.V.-C.)
3 Center for Research in Physical and Mathematical Sciences, Universidad Autónoma de Nuevo Leon,
  San Nicolás de los Garza 66455, Nuevo Leon, Mexico; hector.leijagt@uanl.edu.mx
4 Department of Anatomic Pathology and Cytopathology, University Hospital "Dr. José Eleuterio González",
  Universidad Autónoma de Nuevo Leon, Monterrey 66460, Nuevo Leon, Mexico;
  rodolfo.francomrqz@uanl.edu.mx
5 Department of Hematology, University Hospital "Dr. José Eleuterio González", Universidad Autónoma de
  Nuevo Leon, Monterrey 66460, Nuevo Leon, Mexico; nidia.moncadas@uanl.edu.mx
6 Department of Gynecology and Obstetrics, University Hospital "Dr. José Eleuterio González",
  Universidad Autónoma de Nuevo Leon, Monterrey 66460, Nuevo Leon, Mexico;
  abel.guzmanlp@uanl.edu.mx
* Correspondence: elsa.garzatr@uanl.edu.mx (E.N.G.-T.); mario.simentalme@uanl.edu.mx (M.S.-M.);
  Tel.: +52-81-83294173 (E.N.G.-T.)

Abstract: Articular cartilage lesions are challenging to regenerate, prompting the investigation of novel biomaterial-based therapeutic approaches. Extracellular matrix (ECM)-derived biomaterials are a promising option for this purpose; however, to date, the combination of amniotic membrane (AMM) and articular cartilage (ACM) has not been tested. This study evaluated different concentrations of soluble extracts from the decellularized ECM of amniotic membrane (dAMM) and articular cartilage (dACM), both individually and in combination, to determine their ability to maintain the chondrogenic phenotype in human chondrocytes. After the decellularization process 90–99% of the cellular components were removed, it retains nearly 100% of type 2 collagen and 70% of aggrecan (ACAN) for dACM, and approximately 90% of type IV collagen and 75% of ACAN for dAMM. The biological activity of soluble extracts from dACM and dAMM were evaluated on human chondrocytes. After 72 h, 1.5 mg/mL of dACM and 6 mg/mL of dAMM significantly increased ($p < 0.05$) the proliferation and expression of SOX9 and ACAN. Also, the combination of both (1.5 mg/mL dACM and 6 mg/mL dAMM) showed synergistic effects, enhancing chondrocyte proliferation, maintaining chondrogenic lineage, and increasing the production of cartilage ECM components, such as COLII (1.5-fold), SOX9 (2-fold), and ACAN (2-fold). These results suggest that the combined use of dACM and dAMM has potential for cartilage regeneration.

Keywords: articular cartilage; amniotic membrane; fibrin scaffold; tissue engineering; chondrocyte; ECM-derived biomaterials

1. Introduction

Articular cartilage injury poses a significant challenge in orthopedics due to its limited self-repair capacity, often leading to conditions like osteoarthritis if left untreated [1]. In response, innovative therapeutic strategies such as tissue engineering, regenerative medicine,

and cell therapy, often in conjunction with biomaterials, have emerged as promising approaches for addressing such injuries [2]. Among these, biomaterials derived from the extracellular matrix (ECM) have garnered attention for their biomimetic properties, closely resembling the native tissue ECM composition [3].

The ECM is a complex structure containing bioactive molecules critical for maintaining tissue integrity and function [4]. ECM-based biomaterials provide an ideal microenvironment for cell adhesion, proliferation, and differentiation, and they contain growth factors and signaling molecules that facilitate tissue repair and regeneration [5,6]. These biomaterials also exhibit excellent biocompatibility and cytocompatibility, essential for various biomedical applications [6]. However, the presence of cellular components in ECM-based materials can trigger immune responses and implant rejection, necessitating decellularization [7].

Decellularized ECMs (dECM) derived from different sources, such as porcine liver [8], porcine kidney [9], rat pancreas [10], spinal cord meninges [11], tendon [12], periodontal ligament [13], and others, including amniotic membrane [14,15] and articular cartilage, have shown promise in tissue regeneration [16]. The decellularization process aims to remove cells while preserving the native ECM architecture and bioactive components [17]. Despite their potential in cartilage repair, challenges remain, such as managing inflammatory responses associated with these matrices and limited availability of healthy tissues for decellularization [18,19].

Decellularized articular cartilage ECM (dACM) has gained attention for its ability to retain tissue-specific proteins and bioactive molecules crucial for cartilage regeneration, even after cellular removal [20]. Biofunctionalized dACM scaffolds have demonstrated success in recruiting host cells and promoting chondrogenic differentiation, showing promise for in situ cartilage regeneration [21]. Similarly, decellularized amniotic membrane ECM (dAMM) is notable for its regenerative capabilities in promoting chondrocyte proliferation and cartilage repair [22]. The unique composition of dAMM, including hyaluronic acid, proteoglycans, and growth factors like EGF and bFGF, supports chondrocyte function and enhances cartilage repair strategies [23,24].

Despite their individual successes, the combined effects of dACM and dAMM have not been thoroughly studied, either in vitro or in vivo. This study aims to evaluate the individual and combined effects of dECM derived from articular cartilage and amniotic membrane on maintaining the chondrogenic phenotype of human chondrocytes. This research seeks to elucidate whether combining these biomaterials can enhance their therapeutic potential for cartilage repair and regeneration.

The aim of this work was to study the biological activity of an ECM decellularized from articular cartilage (dACM) and another from amniotic membrane (dAMM) individually and in combination on human chondrocytes. The method of decellularization used detergents and hypotonic buffers, then lyophilization and pulverization. We evaluated particle size by SEM, and the process of decellularization was validated by DAPI fluorescence staining and H and E staining. Preservation of key ECM components such as collagens and glycosaminoglycans was carried out through histological staining, and we evaluated the percentage retention of type 2 collagen and aggrecan by IH and validated it by FT-IR. The biological activity of the soluble extract of the matrices (dACM and dAMM) was evaluated individually and in combination in vitro on human chondrocytes at 24, 48, and 72 h by cell proliferation assays and expression of chondrogenic genes (SOX9, COL-II, ACAN and RUNX2).

2. Materials and Methods

2.1. Human Cartilage Collection and Preparation of Decellularized Articular Cartilage Matrix (dACM)

Human articular cartilage slices (thickness = 2 mm) were obtained from cadaveric donors in an aseptic environment (Research Ethical Committee approval number BI23-001). The cartilage was collected from the areas of the condyles, patella, and femoral trochlea

using a No. 24 scalpel (SensiMedical, Aventura, FL, USA). The cartilage slices were washed three times with PBS (1×, Gibco, Grand Island, NY, USA) containing an Antibiotic–Antimycotic solution (100×, 10,000 units/mL of penicillin, 10,000 μg/mL of streptomycin, and 25 μg/mL of Amphotericin B, Gibco, USA). The slices were then stored at −80 °C until use.

The decellularization protocol was performed on cartilage from 20 donors as previously described by Perez-Silos [25]. Briefly, 205 g of articular cartilage was exposed to five cycles of thermal shock in liquid nitrogen for 5 min, followed by a wash in PBS (1X, Gibco, USA) for 10 min. The cartilage was then crushed with a blender. The pulverized cartilage was washed for 24 h in 10 volumes of hypotonic buffer (10 mM TRIS-HCl, 2 mM EDTA, pH 8) supplemented with 100 mM KCl (99%, SIGMA-ALDRICH, St. Louis, MO, USA) and 5 mM $MgCl_2$ (98%, SIGMA-ALDRICH, USA). Next, 10 volumes hypotonic buffer supplemented with 100 mM KCl, 5 mM $MgCl_2$, and 0.5% SDS (99%, SIGMA-ALDRICH, USA) was added for 18 h. Finally, the matrix was washed with 10 volumes of hypotonic buffer containing 0.5% SDS for 36 h. Following sterile PBS rinsing to eliminate the remaining SDS (3 times), the samples were immediately frozen at −80 °C. The samples were lyophilized for 24 h to completely remove interstitial fluid, followed by fine pulverization using a K10 pulverizer mill (Micron, Shanghai, China) and a Freezer/mill 6870 (SPEX® SamplePrep, Metuchen, NJ, USA). The decellularized articular cartilage matrix (dACM) was then sterilized with ethylene oxide and stored at −80 °C until use. The experimental strategy we followed in this study is shown in Figure 1.
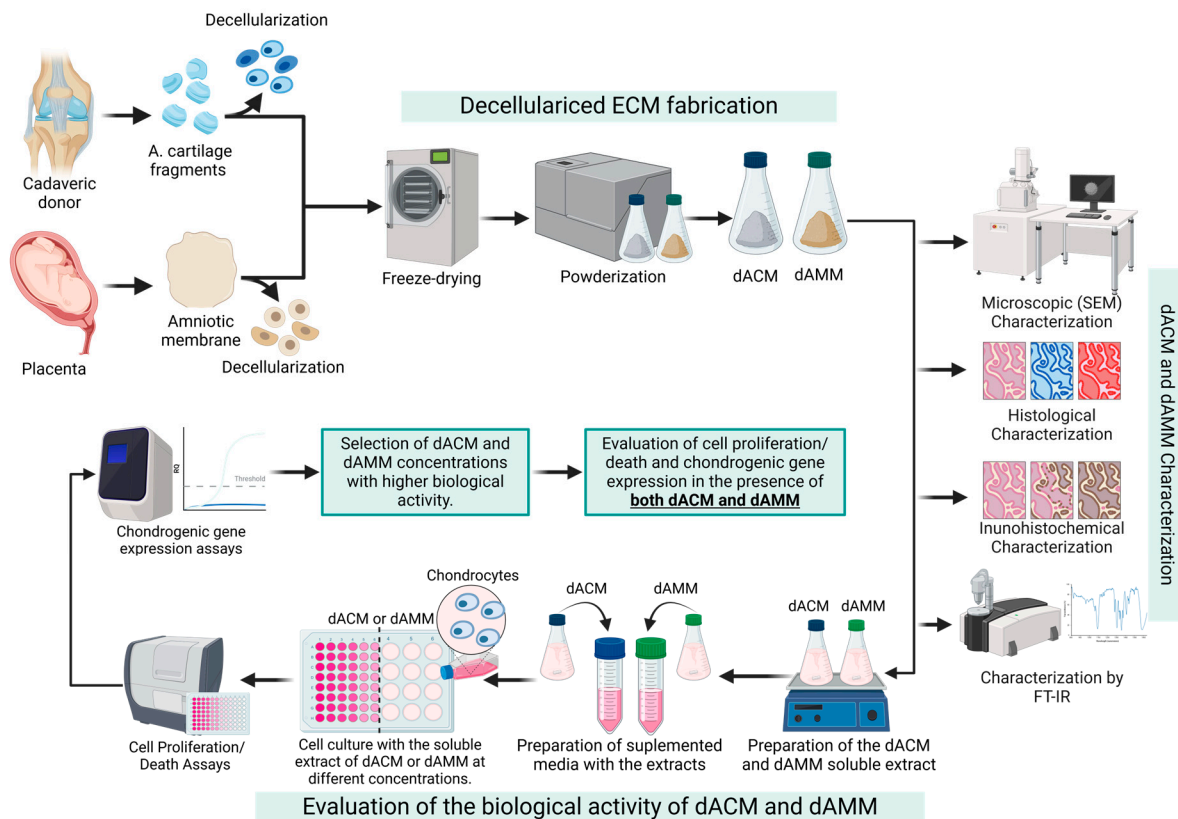
Figure 1. Experimental strategy of the study. Created with BioRender.com.

2.2. Amniotic Membrane Collection and Preparation of Decellularized Amniotic Membrane Matrix (dAMM)

After obtaining informed consent, the surgical intervention was performed. Human placentas were taken from the toco-surgery operating room (Research Ethical Committee approval number BI23-001). The samples were collected and transported at 4 °C in 50 mL sterile tubes containing PBS with Antibiotic–Antimycotic solution (100×, 10,000 units/mL

of penicillin, 10,000 µg/mL of streptomycin, and 25 µg/mL of Amphotericin B, Gibco, USA). In a sterile environment and after three washes with PBS, the samples were cut into pieces of approximately 1 cm^2 and immediately stored at -80 °C until use. A total of 30 amniotic membranes were collected.

The decellularization protocol for the amniotic membrane was performed on the 30 collected membranes (125 g), as described previously by Villamil et al. (2019) [26]. Briefly, all amniotic membranes underwent five freezing cycles in liquid nitrogen (-196 °C) for 30 min, followed by thawing in a serological bath (Precision Scientific Inc., Chicago, IL, USA) at 37 °C for 30 min. The membranes were then treated with 0.1% Tween 80 (SIGMA-ALDRICH, USA) for 4 h, soaked in 0.1 M NaOH (97%, JALMEX, Guadalajara, México) for 1 h, and treated with 0.15% peracetic acid (PAA, 15%, Cetik, Cualiacán, México) in ethanol (96%, CTR, Monterrey, México). The membranes were bleached with NaOH 0.1 M for 1 h and PAA 0.15% for another hour. A final wash with 70% ethanol was applied for 1 h to remove residual nucleic acids and phospholipids from the tissue. Finally, all ethanol was eliminated by washing with PBS for 2 h (three times), and the membranes were stored at -80 °C. Throughout the process, the membranes were gently agitated to ensure a homogeneous wash and minimal damage to the tissue ultrastructure. The amniotic membranes were then lyophilized for 24 h to completely remove liquids, followed by fine pulverization using a K10 pulverizer mill (Micron, Shanghai, China) and a Freezer/mill 6870 (SPEX® SamplePrep, Metuchen, NJ, USA). The decellularized amniotic membrane matrix (dAMM) was sterilized with ethylene oxide and stored at -80 °C until use.

2.3. Histological and Immunohistochemical Analyses

Both the dACM and dAMM were fixed in 4% PFA for 24 h, then embedded in paraffin blocks using conventional histological methods. Subsequently, 4 µm histological sections were prepared and stained with various dyes for different analyses. To evaluate DNA, nuclear, or cell remnants on the matrices, 4′,6-diamidino-2-phenylindole (DAPI, VECTOR, Newark, CA, USA) staining was used. Hematoxylin and eosin (H and E) staining examined the general histology of the samples. Safranin O staining detected the presence of sulfated proteoglycans, while Masson's trichrome staining visualized collagen fibers in the ECM.

The conservation of ECM components, such as type II collagen fibers and aggrecans, was analyzed by immunohistochemistry (IHC). Primary antibodies, anti-col II (dilution 1:400, ab34712, ABCAM, Cambridge, UK), and anti-aggrecan (dilution 1:100, ab3778, ABCAM, Cambridge, UK) were used and incubated at 4 °C overnight. The mouse- and rabbit-specific detection system HRP/DAB (ABC) detection IHC kit (ab64264m, ABCAM, Waltham, MA, USA) was employed, with Gill's hematoxylin (SIGMA-ALDRICH, USA) as a counterstain. Negative controls for the IHC were samples of articular cartilage without the primary antibody. Images were captured with an Olympus AX70 microscope (Olympus, Tokyo, Japan). For analysis, 10 fields per slide (3 slides per tissue) were examined to calculate the respective antibody-positive area percentage using ImageJ software Version 1.54g.

2.4. dACM and dAMM Microstructure Analysis

The lyophilized dACM and dAMM were sputter-coated with gold and transferred to a scanning electron microscope (SEM) (JSM-6390LV, JEOL, Tokyo, Japan). The particle size was then measured through image analysis.

2.5. FT-IR Spectroscopy

The Fourier transform infrared spectroscopy (FT-IR) spectral profiles of dACM and dAMM were obtained using a PerkinElmer Frontier spectrometer in a spectral range of 400–4000 cm^{-1}. This analytical approach allowed for the detailed examination of the molecular composition and structural characteristics of the samples.

2.6. Chondrocytes Isolation and Cuture

Chondrocytes were isolated from the knee joints of healthy human donors and cadaveric donors (Research Ethical Committee approval number BI23-001). Briefly, the articular cartilage tissue was cut into small pieces (<1 mm) and incubated with 2.5% trypsin (Gibco, USA) at 37 °C for 30 min. Following the removal of the trypsin solution, the tissue was digested with 2 mL of 0.2% type II collagenase (Gibco, USA) at 37 °C for 2 h. Released cells were obtained by centrifugation at 4000 rpm for 10 min, and the remaining tissue was digested one more time for 90 min. The cells were cultured in Dulbecco's Modified Eagle's Medium (DMEM; Gibco, USA) supplemented with 10% FBS (Gibco, USA) containing Antibiotic–Antimycotic solution (100×, 10,000 units/mL of penicillin, 10,000 μg/mL of streptomycin, and 25 μg/mL of Amphotericin B, Gibco, USA). The medium was replaced every 2 days. Once the cells reached 80%–90% confluence, the chondrocytes were used for all subsequent experiments. Chondrocytes with more than 3 passages were not used.

2.7. In Vitro Cell Culture Assays

The soluble extract of decellularized ECM was prepared by incubating 200 mg of dACM or dAMM with 2 mL of serum-free OptiMEM (Gibco, USA) at 37 °C for 24 h. Following the incubation period, the medium was cleared by centrifugation at 4000 rpm for 20 min; then, the supernatant medium was diluted with 5% FBS OptiMEM to the concentrations of 15 mg/mL, 7.5 mg/mL, 1.5 mg/mL, and 0.15 mg/mL of dACM (Dry weigh), as described by [27], and 12 mg/mL, 6 mg/mL, 3 mg/mL, and 0.3 mg/mL of dAMM (Dry weigh), as described by [28], and stored at −20 °C or used immediately. For cellular proliferation and cytotoxicity assays, 5×10^3 chondrocytes were seeded per well in a 96-well plate with 100 μL/well OptiMEM supplemented with 5% FBS. After 24 h of incubation, the medium was removed, and the cells were treated with 100 μL/well of the medium at the different concentrations of the soluble extract of dACM or dAMM. The cells were then incubated for 24, 48, and 72 h. ATP luminescence was determined using CellTiter-Glo (Promega, Madison, WI, USA) to evaluate proliferation. A CellTiter-Glo reagent (100 μL) was added to each well, agitated for 2 min at 300–500 rpm, and incubated for 10 min at room temperature. Luminescence was quantified using a Cytation 3 plate reader (BioTek, Winooski, VT, USA). The percentage of cell death was calculated using the following formula:

$$1 - \frac{\text{treatment mean luminescence}}{\text{treatment mean luminescence}} \times 100$$

2.8. Chondrogenic Gene Expression

The chondrocytes were seeded into a 24-well plate at 1×10^5 cells/well with OptiMEM supplemented with 5% FBS. After 24 h of incubation, the cells were treated with the soluble extract at concentrations of 15 mg/mL, 7.5 mg/mL, 1.5 mg/mL, and 0.15 mg/mL for dACM, and 12 mg/mL, 6 mg/mL, 3 mg/mL, and 0.3 mg/mL for dAMM. The cells were then incubated for 24, 48, and 72 h.

RNA isolation was carried out using the RNeasy Mini Kit (Qiagen, Germantown, MD, USA) according to the manufacturer's protocol. Reverse transcription of total RNA to single-stranded cDNA was completed using the SuperScript™ III First-Strand Synthesis System kit (Invitrogen, Carlsbad, CA, USA) following the manufacturer's instructions. Gene expression was analyzed using a 7500 real-time PCR system (Applied Biosystems, Waltham, MA, USA). TaqMan probes, purchased from Applied Biosystems, included several target genes: Beta-2 microglobulin (B2M: endogenous control; ID: Hs99999907_m1), aggrecan (ACAN; ID: Hs00153936_m1), SRY (sex-determining region Y)-box 9 (SOX9; ID: Hs00165814_m1), type II collagen (COL2A1; ID: Hs00156568_m1), and RunX2. Data from 3 samples were evaluated as mRNA levels in triplicate. The $2^{-\Delta\Delta Ct}$ method was used to calculate the relative expression (RQ) of each target gene.

2.9. Statistical Analysis

All experiments were performed in triplicate and repeated three times. Statistical analysis was conducted using GraphPad Prism 9.0.2 software. First, the Shapiro–Wilk test was performed to evaluate the normal distribution of the quantitative variables including results from decellularization, morphometric analysis, relative gene expression, and cell proliferation. Afterward, an unpaired *t*-test with Welch's correction was used to evaluate significant differences in such quantitative analyses. Data are presented as mean and standard deviation (SD). Statistical significance was set at * $p < 0.05$, ** $p < 0.01$, *** $p < 0.001$.

3. Results

3.1. Particle Sizes and Assays to Evaluate the Decellularized Process

After the decellularization, lyophilization, and pulverization of the articular cartilage and amniotic membrane, fine whitish powder for dACM (Figure 2A), and slightly coarser yellowish powder for dAMM (Figure 2D) were obtained. Scanning electron microscopy analysis revealed that both matrices exhibited a porous structure with varying particle sizes. The particle size of dACM ranged from 1.6 to 600 μm (Figure 2B,C), while for dAMM, it ranged from 0.3 to 1700 μm (Figure 2E,F).
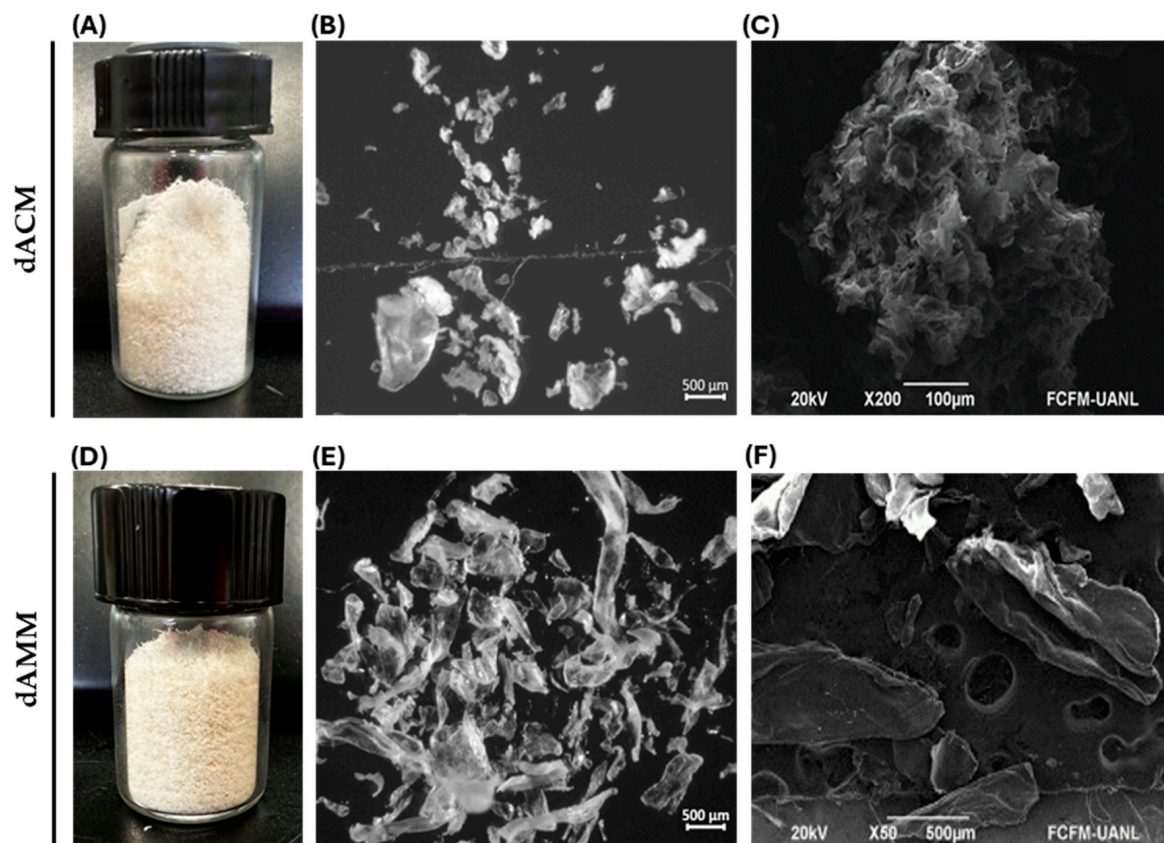

Figure 2. Macroscopic and microscopic description of dACM and dAMM: (**A**) Macroscopic photography of dACM; (**B**) scanning electron micrography image at 50× of dACM; (**C**) scanning electron micrography image at 20,000× of dACM; (**D**) macroscopic photography of dAMM; (**E**) scanning electron micrography image at 200× of dAMM; (**F**) scanning electron micrography image at 2000× of dAMM.

To assess the degree of decellularization, DAPI staining and H and E staining were conducted. The staining showed residual nuclei in the ECM of both tissues (Figure 3A,F). Image analysis indicated that dACM had less than 5% residual nuclei compared to native cartilage (Figure 3E), whereas dAMM was nearly completely decellularized, with only about 1% residual nuclei compared to native amniotic membrane (Figure 3J). H and E staining further revealed the absence of chondrocyte nuclei in decellularized cartilage

(Figure 3B) and the lack of epithelial cell nuclei in decellularized amniotic membrane (Figure 3G). The decellularization process eliminated over 90% of cells in both dACM and dAMM, as evidenced by the staining results.
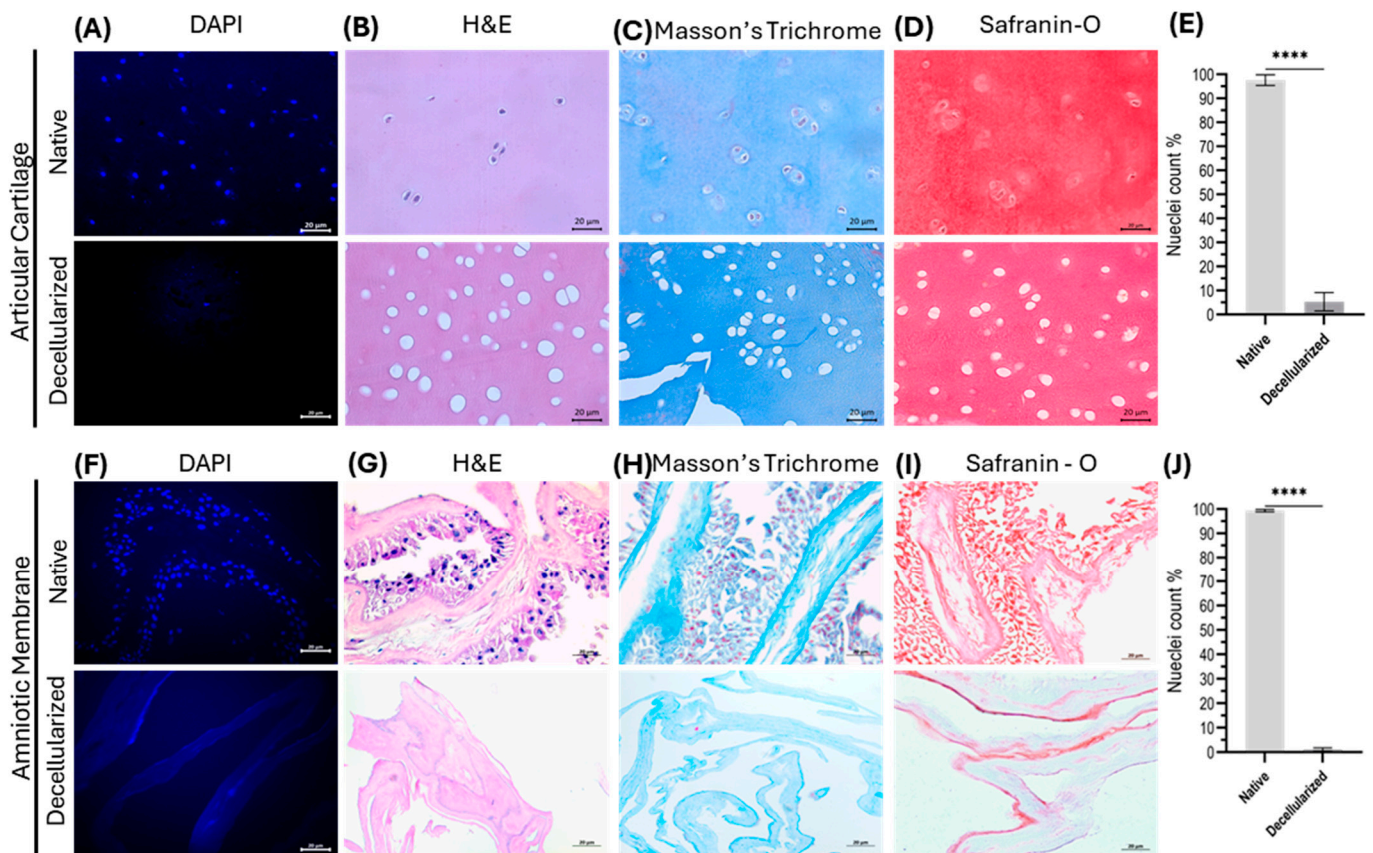

Figure 3. Histological characterization of articular cartilage (AC) and amniotic membrane (AM) before and after decellularization. (**A**) DAPI staining of AC; (**B**) hematoxylin and eosin staining of AC; (**C**) Masson's trichrome staining of AC; (**D**) Safranine O staining of AC; (**E**) quantification of AC decellularization; (**F**) DAPI staining of AM; (**G**) hematoxylin and eosin staining of AM; (**H**) Masson's trichrome staining of AM; (**I**) Safranine O staining of AM; (**J**) quantification of AM decellularization. **** = t test p value $\leq$ 0.0001.

3.2. Preservation of the Native Structure before and after Decellularized Process

To ensure that the chemical decellularization and mechanical pulverization processes did not alter the essential extracellular matrix (ECM) components of the tissues, a comprehensive histological and immunohistochemical characterization was conducted. Histological analysis using H and E staining confirmed the preservation of the ECM structure of both cartilage (Figure 3B–D) and amniotic membrane (Figure 3G–I). Eosin binding to ECM components was observed in both native and decellularized tissues. Masson's trichrome staining further demonstrated the presence of collagens in the decellularized ECMs, indicated by a blue color characteristic of aniline blue in both cases (Figure 3C for cartilage and Figure 3H for amniotic membrane).

Safranin staining was employed to assess the preservation of aggrecans. While no differences were noted in the cartilage before and after decellularization (Figure 3D), a decrease in staining intensity was observed in the decellularized amniotic membrane (Figure 3I).

Immunohistochemical staining for type 2 collagen and aggrecan was performed with semi-quantitative analysis (Figure 4A,B for cartilage and, Figure 4E,F for amniotic membrane). The results showed that dACM retained nearly 100% of the type 2 collagen found in native cartilage (Figure 4C), but there was a 30% decrease in aggrecan compared

to native tissue (Figure 4D). For dAMM, approximately 89% of type IV collagen and almost 75% of aggrecan were retained (Figures 4G and 4H, respectively).
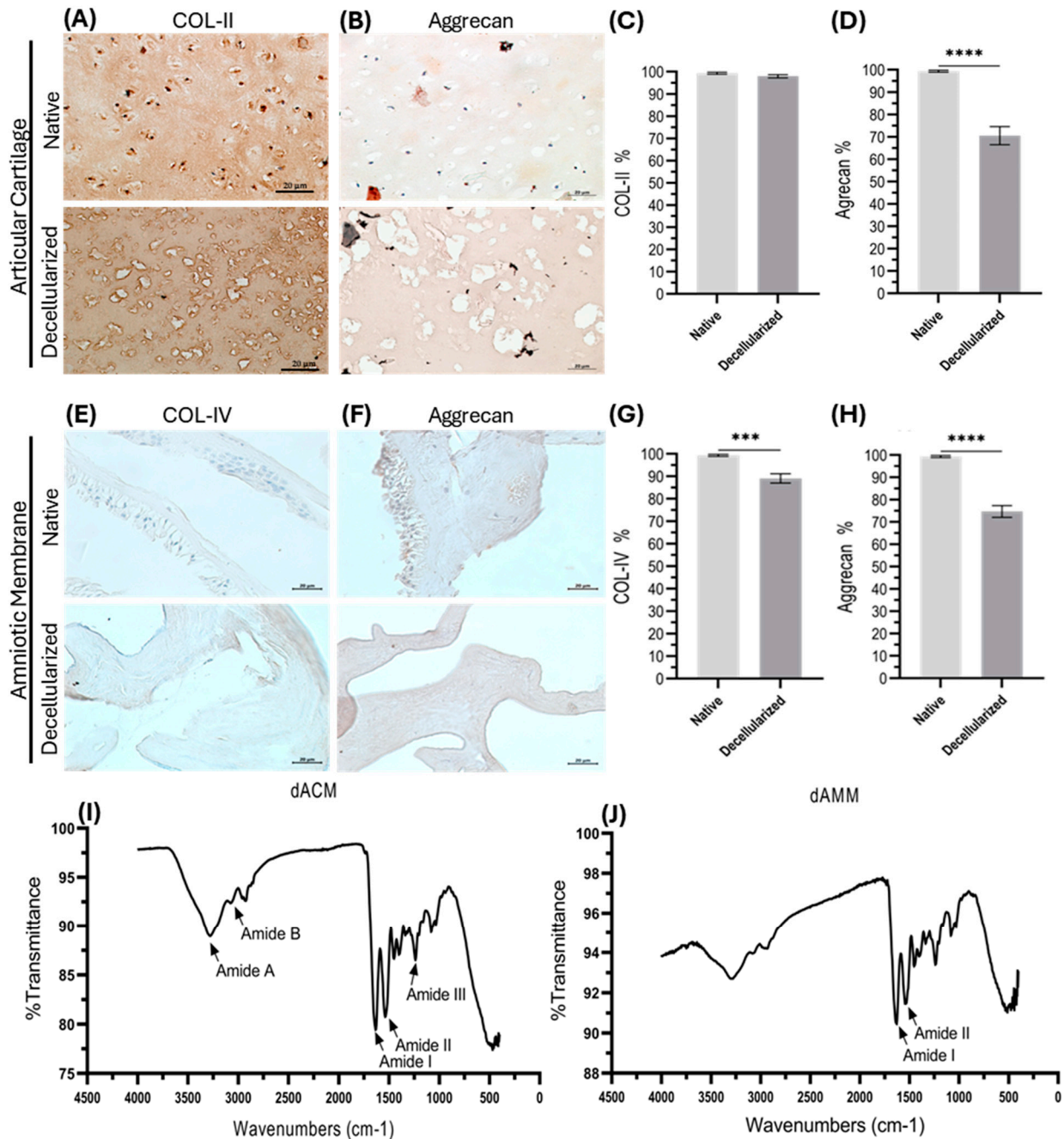

Figure 4. Characterization of articular cartilage (AC) and amniotic membrane (AM) before and after decellularization. (**A**) anti-col II IHC of AC; (**B**) anti-aggrecan IHC of AC; (**C**) quantification of collagen conservation of AC; (**D**) quantification of aggrecan conservation of AC; (**E**) anti-col IV IHC of AM; (**F**) anti-aggrecan IHC of AM; (**G**) quantification of collagen conservation of AM; (**H**) quantification of aggrecan conservation of AM; (**I**) dACM FT-IR spectrum; (**J**) dAMM FT-IR spectrum. *** = t test p value $\leq$ 0.001; **** = t test p value $\leq$ 0.0001.

To validate the preservation of the main component collagen, Fourier transform infrared (FT-IR) spectroscopy was utilized to identify the main components in the matrices.

The FT-IR spectra of dACM revealed peaks associated with structural type II collagen amides A, B, I, II, and III (Figure 4I). On the other hand, the FT-IR spectrum of dAMM exhibited peaks corresponding to type IV collagen (Figure 4J). Overall, the comprehensive

characterization through histological, immunohistochemical, and FT-IR analyses confirmed the successful preservation of essential ECM components in both dACM and dAMM.

3.3. Proliferative Effect of Individually Soluble Extracts from dACM and dAMM on Human

After confirming the preservation of essential components relevant to the cartilage regeneration environment, the effects of both extracellular matrices (ECMs) on chondrocytes were analyzed to determine the concentration that elicits the greatest biological effect.

The assays revealed that the dACM and dAMM extracts can induce chondrocyte proliferation. At 24 and 48 h, no significant differences were observed compared to the negative control. However, after 72 h of culture, the dACM extract at all concentrations demonstrated the highest proliferation and viability rates in chondrocytes ($p < 0.001$), as depicted in Figure 5A. Similarly, dAMM showed no effect at 24 h, but at 48 h, treatment with dAMM extract at concentrations of 6 and 12 mg/mL increased the number of cells ($p < 0.05$). Notably, at 0.3 mg/mL, the cell count increased by almost 30%, resulting in significant differences compared to the control ($p < 0.001$). By 72 h, all evaluated concentrations showed a 40% increase in the number of cells compared to the control, as illustrated in Figure 5D ($p < 0.05$).

3.4. Evaluation of the Expression Level of Chondrogenesis-Related Markers

At 24 h, the dACM extract at concentrations of 0.15 and 1.5 mg/mL significantly increased SOX9 expression. At 48 h, a higher SOX9 expression was observed at concentrations of 1.5, 7.5, and 15 mg/mL compared to the untreated control group. Interestingly, at 72 h, the group treated with 1.5 mg/mL dACM showed the highest expression of SOX9, with levels almost three times higher than the untreated control group (Figure 5B).

Conversely, the dAMM extract increased SOX9 expression in all groups, with a significant difference observed at 6 mg/mL compared to the control. At 48 h, concentrations of 6 and 12 mg/mL significantly increased SOX9 expression by almost 6-fold. At 72 h, a decrease in SOX9 expression was further observed, although concentrations of 3 and 6 mg/mL still showed higher expression levels than the control group (Figure 5E).

Analysis of ACAN expression showed that only the dACM at 1.5 mg/mL increased the expression of this gene at 24, 48, and 72 h ($p < 0.05$) (Figure 5C). On the other hand, ACAN expression levels were increased in the presence of dAMM at 24 h, with all concentrations showing higher expression levels than the control group. Significant differences were observed at concentrations of 3 and 6 mg/mL. At 72 h, ACAN expression decreased, but concentrations of 3, 6, and 12 mg/mL still showed significantly higher expression levels compared to the control group. (Figure 5F).

Interestingly, the dACM extract did not induce RUNX2 expression in any of the treated groups. In contrast, the dAMM extract increased RUNX2 expression at 24 h, but this effect was not sustained at 48 and 72 h (Figure 5G).

3.5. Analysis the Combination of dACM and dAMM on Cell Proliferation and Chondrogenic Gene Expression

To assess the combined effect of dACM and dAMM, concentrations were selected based on previous experiments that demonstrated a higher proliferative index and increased levels of SOX9 and ACAN expression in chondrocytes. The concentrations chosen were 1.5 mg/mL of dACM and 6 mg/mL of dAMM. The mixture of these matrices significantly increased cell proliferation after 24, 48, and 72 h, showing notable differences compared to the controls ($p < 0.001$). Meanwhile, at 72 h, the dACM control exhibited a higher percentage of live cells than the mixture; the cell counts in the mixture remained consistently higher than the control (Figure 6A).
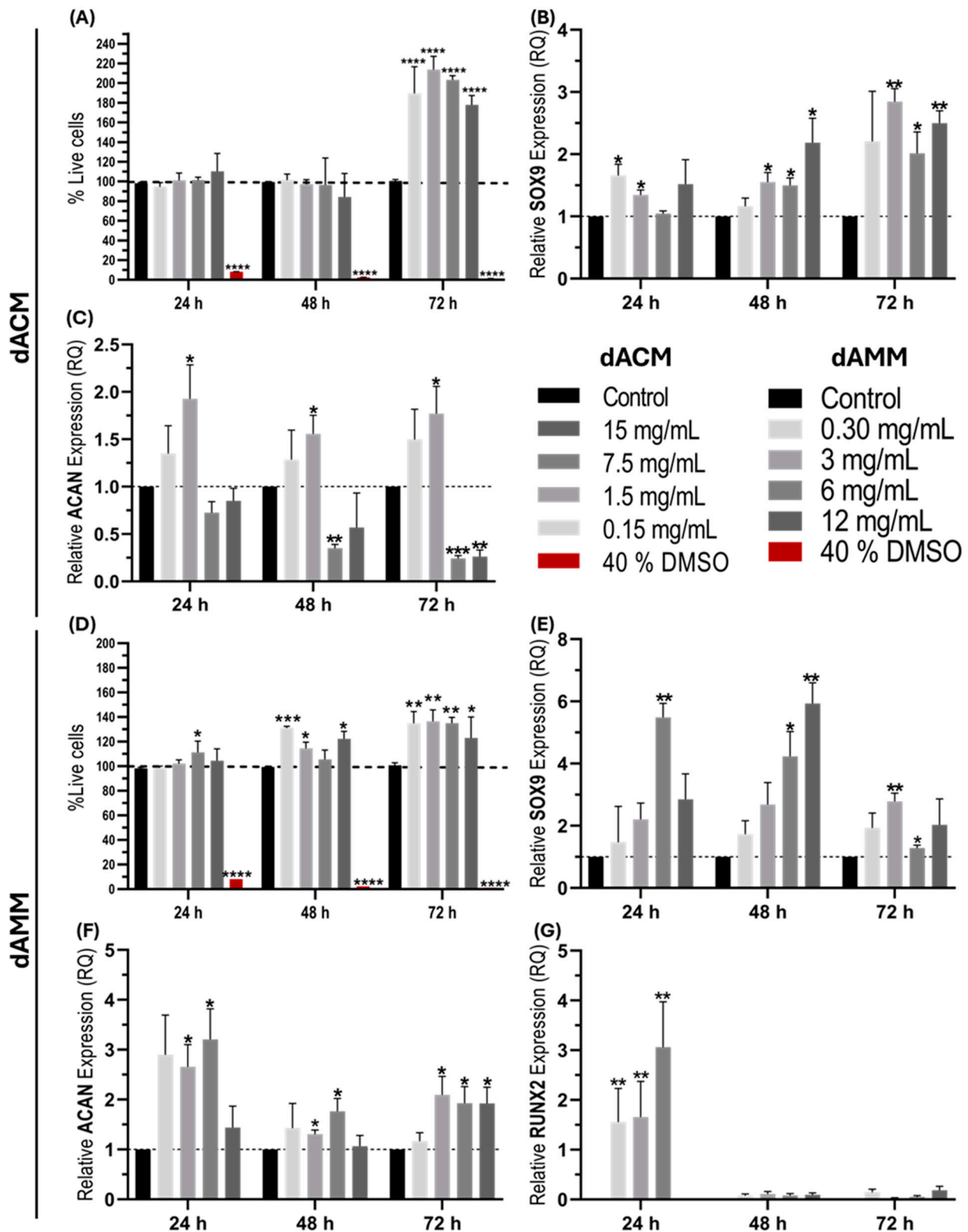
Figure 5. Effect of dACM and dAMM on in vitro chondrocytes culture: (**A**) effect of dACM on cell proliferation; (**B**) effect of dACM on SOX9 expression; (**C**) effect of dACM on ACAN expression; (**D**) effect of dAMM on cell proliferation; (**E**) effect of dAMM on SOX9 expression; (**F**) effect of dAMM on ACAN expression; (**G**) effect of dACM on RUNX expression. * = *t* test *p* value ≤ 0.05; ** = *t* test *p* value ≤ 0.005; *** = *t* test *p* value ≤ 0.001; **** = *t* test *p* value ≤ 0.0001.
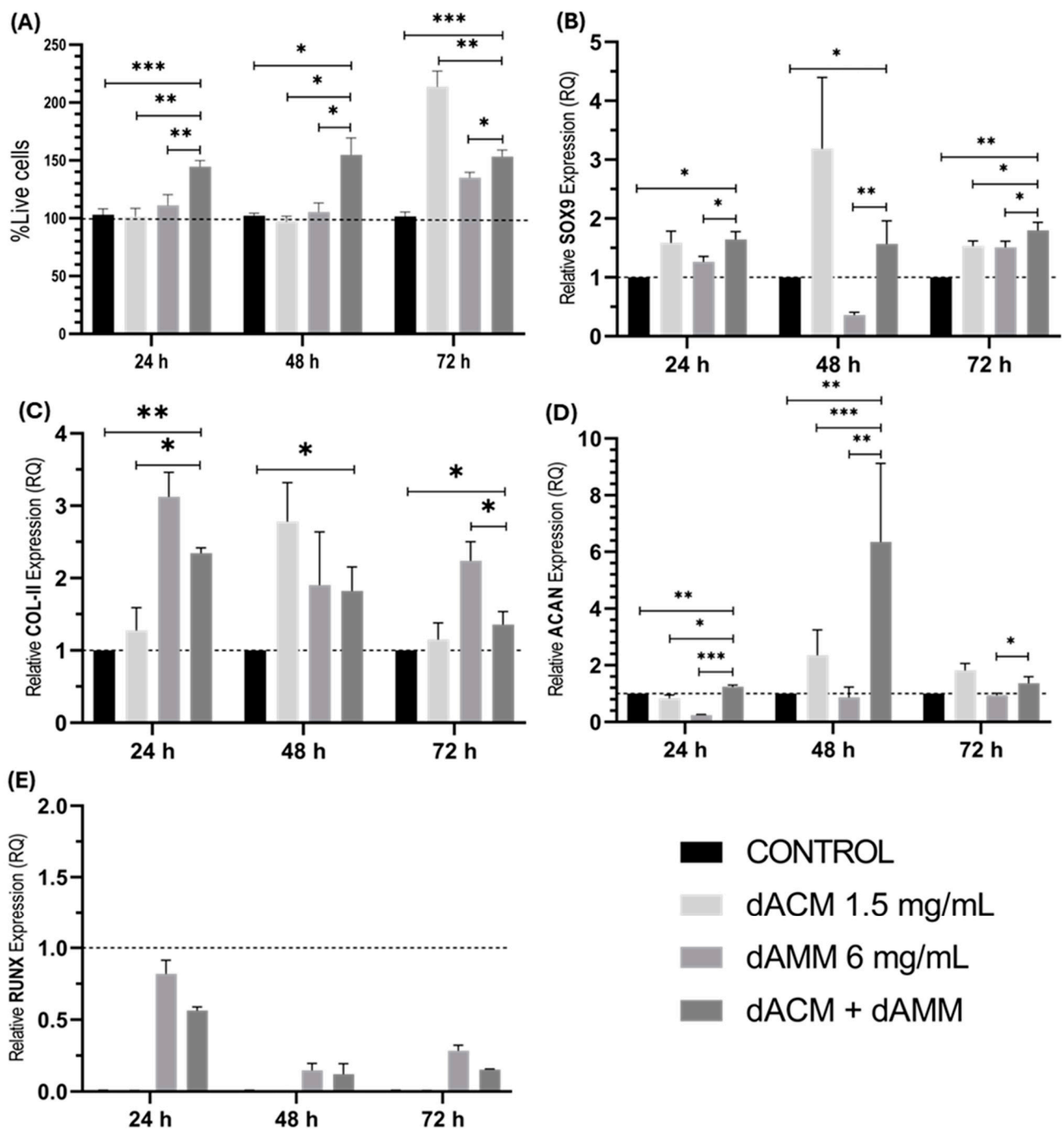
Figure 6. Effect of the mixture of dACM and dAMM on in vitro Chondrocytes culture: (**A**) effect of dACM + dAMM on cell proliferation; (**B**) effect of dACM + dAMM on SOX9 expression; (**C**) effect of dACM + dAMM on COL-II expression; (**D**) effect of dACM + dAMM on ACAN expression; (**E**) effect of dACM + dAMM on RUNX expression. * = t test p value ≤ 0.05; ** = t test p value ≤ 0.005; *** = t test p value ≤ 0.001.

In the presence of both matrices, SOX9 expression at 24 and 48 h surpassed that of groups treated with only dACM or dAMM, as well as the untreated control ($p < 0.05$). At 48 h, the mixed group displayed the highest SOX9 expression, significantly differing from both the control group and the group treated with dAMM alone. However, by 72 h, a higher SOX9 expression was observed after treatment with dAMM (Figure 6B). The combination of both matrices increased COL-II expression at 24, 48, and 72 h; however, this expression decreased with time, and at 72 h, the mixture showed significant differences

with respect to the untreated control and dAMM group (Figure 6C). At 48 h, dAMM exhibited higher ACAN expression compared to dACM; nevertheless, by 72 h, the mixed group displayed the highest ACAN expression compared to the untreated control or either dACM or dAMM alone (Figure 6D). Notably, all experiments involving dACM and dAMM, either individually or in combination, showed reduced expression of RUNX, an osteogenic marker.

4. Discussion

In this study, we generated two decellularized biological matrices: one from articular cartilage (dACM) and the other from amniotic membrane (dAMM). Both matrices exhibited biological activity and a high content of biomolecules associated with cartilage generation.

Decellularized extracellular matrices (ECMs) have been extensively utilized in tissue engineering to treat tissue injuries by preventing scar formation and promoting regeneration [29]. They have garnered significant attention for their ability to maintain biological activity, preserve growth factors, and important proteins following chemical/physical decellularization processes. In tissue engineering, native-tissue-derived ECMs are often pulverized into powders that can be further processed into various forms, such as hydrogels, foams, nanofibers, coatings, and 3D-printed constructs [30]. This versatility in processing powdered ECM allows for the fabrication of scaffolds tailored to specific tissue-engineering needs, promoting tissue regeneration [3]. In this work, we assess the potential of blending dACM and dAMM for use in cartilage engineering.

A fundamental aspect of working with biological tissues is ensuring complete removal of cellular components. There are three essential criteria for successful tissue decellularization: (a) the decellularized ECM should contain less than 50 ng/mg dry tissue of dsDNA, (b) any remaining DNA fragments should be smaller than 200 base pairs, and (c) the decellularized ECM should show no visible nuclear material when stained with DAPI or hematoxylin and eosin [31,32]. In our study, dACM showed over 95% decellularization, with no observed nuclei in DAPI or H and E staining, consistent with other reported protocols using varying decellularization times and methods [26,27,33]. dAMM achieved almost complete removal (99.5%) of cellular components, similarly showing no visible nuclei in staining. However, to fully meet the third criterion, future studies should include DNA concentration analysis in the decellularized matrices, which was not performed in our study.

Decellularization techniques are crucial for removing cellular components while preserving ECM proteins and glycosaminoglycans [31,34], thereby maintaining the structural and functional properties essential for regenerative potential [35]. Furthermore, preservation of protein–GAG and protein–protein interactions during decellularization processes helps maintain ECM's native structure [31]. Our matrices retained major components such as type II collagen and aggrecan, as confirmed by histological staining and immunohistochemistry. While collagen preservation was nearly 100% in both matrices, a significant loss of aggrecan during decellularization was noted, likely due to its localization on hyaluronan molecules within the ECM 3D structure [36]. Nevertheless, retention levels exceeding 70% were observed in both dACM and dAMM, consistent with findings by Guo et al. [37], where collagen preservation was nearly complete, while glycosaminoglycan levels varied depending on the decellularization method [37,38]. The FT-IR analysis confirmed the presence of type II collagen in dACM and type IV collagen in dAMM.

Studies have highlighted the significant influence of ECM particle size on tissue formation and fate, independent of initial biomaterial composition [39,40]. For instance, nanometer-sized ECM particles have been proposed to enhance cellular responses under culture conditions, emphasizing particle size's role in cell proliferation, differentiation, and tissue development [41]. Our matrices exhibited heterogeneous particle sizes, beneficial for scaffold biomechanics, growth factor release, and tissue-derived protein interaction [42]. It was reported that the microarchitecture and bioactivity of porous scaffolds significantly influence cartilage-tissue-engineering outcomes, showing that the scaffold composition

facilitated cartilage maturation and ECM secretion, and controllable pore sizes can induce cartilage regeneration [43].

When we analyzed the soluble extract of the decellularized matrices, we confirmed that our ECM-derived biomaterials have biological activity, as they were able to induce the proliferation of chondrocytes in culture after 48 h [16,23], which are associated with chondrocyte proliferation and maintenance of the chondrogenic lineage. This can be due to presence of soluble growth factors, such as bFGF, insulin-like growth factor-1 (IGF-1), vascular endothelial growth factor (VEGF), transforming growth factor-β1 (TGF-β1), bone morphogenic protein-2 (BMP-2), and growth differentiation factor 7 (GDF-7) in dACM or EGF, KGF, HGF, TGF-β1, TNF-α, EGF, IGF-1, PDGF–BB, HGF, VEGF, and bFGF, which can modulate the bioactivity of dAMM. According to a decellularization protocol applied to decellularized amniotic membrane, detergents, such as triton and hypotonic buffers, and NaOH do not affect the detection of structural proteins, as shown in this work [44,45]. However, the limitation of this study is the lacking characterization of soluble growth factors.

Our results demonstrated that dACM and dAMM were able to increase the expression levels of SOX9 and can maintain the chondrocyte cell lineage. The main component of hyaline cartilage is type 2 collagen; the combination of dACM and dAMM was shown to be able to improve the expression of COL-II in chondrocytes; however, although the dAMM group was shown to induce higher levels at the three measured times and dACM was shown to induce higher levels at 48 h, these show a tendency to decrease the expression with the passage of time; this could indicate that the combination of dACM and dAMM could generate more stable and maintainable results over long periods of time, but further tests are still needed to confirm this. Several authors report a significant increase in COL-II in mesenchymal stem cell cultures when exposed to decellularized matrices for 7 and 14 days [46–48]; however, this may differ from our results because we used an already differentiated cell line, which could influence the COL-II expression patterns, since chondrocytes do not go through a differentiation stage [49]; so, the bioactive components of the extracts could affect the cell line differently.

On the other hand, the expression levels of ACAN changed drastically and increased almost fourfold compared to the treatment with only one decellularized matrix (dAMM), showing an effect on ECM components synthesis. Another beneficial was used because one of the main problems with chondrocytes is that only young cell lines can be used since old cell lines tend to become undifferentiated [50]. Furthermore, as shown by the lack of RUNX2 expression, dACM alone or in combination with dAMM did not promote osteogenic differentiation. Regarding the production of cartilage components, dAMM induced higher levels of ACAN expression compared to dACM. This can be attributed to the higher amounts of TGF-β found in the amniotic membrane compared to articular cartilage [16,23]. Another important point to consider is that in several published works [27,47,48,51,52], decellularized matrices were directly added to scaffolds in 3D cultures. This can delay the release of active components of the matrices and regulate the supply of these active components; so, the effect on the cells is different. Meanwhile, in our approach, all active components are available in the 2D culture, which could explain why most of the genes that were measured (either in the presence of one or another decellularized matrix or both) presented a peak of expression at 48 h and subsequently decreased the expression.

Our results suggest that decellularized matrices derived from articular cartilage and amniotic membrane promote the proliferation and maintenance of the chondrogenic lineage, and the combination of both (dAMM and dACM) has greater potential in the engineering of cartilage tissue. Given their high collagen content, these materials could potentially serve as effective scaffolds, particularly in hydrogel formulations through simple enzymatic digestion. Future research should involve testing these materials in 3D in vitro models followed by in vivo studies

5. Conclusions

According to our results, ECM from articular cartilage and decellularized, pulverized, and freeze-dried amniotic membrane had heterogeneous particle sizes ranging from 1.6 to 600 μm for dAMM and 0.3 to 1700 μm for dACM, as well as preserved essential components of the ECM, such as collagen and ACAN. Biological activity using soluble extracts individually stimulated the proliferation of chondrocytes, and the expression of chondrogenic genes (SOX9, ACAN and COLII) at all evaluated times but were higher after 72 h. We observed the greatest effects with dACM at 1.5 mg/mL and 6 mg/mL for dAMM. The combination of dACM and dAMM showed synergistic effects, improved the expression of chondrogenic markers, and proliferated and increased the production of cartilage extracellular matrix components more than those used individually, suggesting that the combination of dACM and dAMM has potential for the cartilage regeneration.

References

1. Blache, U.; Stevens, M.M.; Gentleman, E. Harnessing the Secreted Extracellular Matrix to Engineer Tissues. *Nat. Biomed. Eng.* **2020**, *4*, 357–363. [CrossRef]
2. Seixas, M.J.; Martins, E.; Reis, R.L.; Silva, T.H. Extraction and Characterization of Collagen from Elasmobranch Byproducts for Potential Biomaterial Use. *Mar. Drugs* **2020**, *18*, 617. [CrossRef]
3. Golebiowska, A.A.; Intravaia, J.T.; Sathe, V.M.; Kumbar, S.G.; Nukavarapu, S.P. Decellularized Extracellular Matrix Biomaterials for Regenerative Therapies: Advances, Challenges and Clinical Prospects. *Bioact. Mater.* **2024**, *32*, 98–123. [CrossRef] [PubMed]
4. Luo, R.; Hu, R.; Xu, J.; Yu, P.; Wu, X.; Zhe, M.; Liu, M.; Xing, F.; Xiang, Z.; Zhou, C.; et al. Decellularized Extracellular Matrix as a Promising Biomaterial for Musculoskeletal Tissue Regeneration. *Nanotechnol. Rev.* **2023**, *12*, 20230151. [CrossRef]
5. Wang, H.; Yu, H.; Zhou, X.; Zhang, J.; Zhou, H.; Hao, H.; Ding, L.; Li, H.; Gu, Y.; Ma, J.; et al. An Overview of Extracellular Matrix-Based Bioinks for 3D Bioprinting. *Front. Bioeng. Biotechnol.* **2022**, *10*, 905438. [CrossRef] [PubMed]
6. Song, M.; Wang, W.; Ye, Q.; Bu, S.; Shen, Z.; Zhu, Y. The Repairing of Full-Thickness Skin Deficiency and Its Biological Mechanism Using Decellularized Human Amniotic Membrane as the Wound Dressing. *Mater. Sci. Eng. C* **2017**, *77*, 739–747. [CrossRef] [PubMed]
7. Nakamura, N.; Kimura, T.; Kishida, A. Overview of the Development, Applications, and Future Perspectives of Decellularized Tissues and Organs. *ACS Biomater. Sci. Eng.* **2017**, *3*, 1236–1244. [CrossRef] [PubMed]
8. Ijima, H.; Nakamura, S.; Bual, R.; Shirakigawa, N.; Tanoue, S. Physical Properties of the Extracellular Matrix of Decellularized Porcine Liver. *Gels* **2018**, *4*, 39. [CrossRef] [PubMed]
9. Hussein, K.H.; Saleh, T.; Ahmed, E.; Kwak, H.H.; Park, K.M.; Yang, S.R.; Kang, B.J.; Choi, K.Y.; Kang, K.S.; Woo, H.M. Biocompatibility and Hemocompatibility of Efficiently Decellularized Whole Porcine Kidney for Tissue Engineering. *J. Biomed. Mater. Res. A* **2018**, *106*, 2034–2047. [CrossRef]

10. Napierala, H.; Hillebrandt, K.H.; Haep, N.; Tang, P.; Tintemann, M.; Gassner, J.; Noesser, M.; Everwien, H.; Seiffert, N.; Kluge, M.; et al. Engineering an Endocrine Neo-Pancreas by Repopulation of a Decellularized Rat Pancreas with Islets of Langerhans. *Sci. Rep.* **2017**, *7*, 41777. [CrossRef]

11. Ozudogru, E.; Isik, M.; Eylem, C.C.; Nemutlu, E.; Arslan, Y.E.; Derkus, B. Decellularized Spinal Cord Meninges Extracellular Matrix Hydrogel That Supports Neurogenic Differentiation and Vascular Structure Formation. *J. Tissue Eng. Regen. Med.* **2021**, *15*, 948–963. [CrossRef] [PubMed]

12. Song, H.; Yin, Z.; Wu, T.; Li, Y.; Luo, X.; Xu, M.; Duan, L.; Li, J. Enhanced Effect of Tendon Stem/Progenitor Cells Combined with Tendon-Derived Decellularized Extracellular Matrix on Tendon Regeneration. *Cell Transpl.* **2018**, *27*, 1634–1643. [CrossRef]

13. Farag, A.; Vaquette, C.; Hutmacher, D.W.; Bartold, P.M.; Ivanovski, S. Fabrication and Characterization of Decellularized Periodontal Ligament Cell Sheet Constructs. *Methods Mol. Biol.* **2017**, *1537*, 403–412. [CrossRef]

14. Kafili, G.; Niknejad, H.; Tamjid, E.; Simchi, A. Amnion-Derived Hydrogels as a Versatile Platform for Regenerative Therapy: From Lab to Market. *Front. Bioeng. Biotechnol.* **2024**, *12*, 1358977. [CrossRef]

15. Hu, Z.; Luo, Y.; Ni, R.; Hu, Y.; Yang, F.; Du, T.; Zhu, Y. Biological Importance of Human Amniotic Membrane in Tissue Engineering and Regenerative Medicine. *Mater. Today Bio* **2023**, *22*, 100790. [CrossRef]

16. Zhang, Q.; Hu, Y.; Long, X.; Hu, L.; Wu, Y.; Wu, J.; Shi, X.; Xie, R.; Bi, Y.; Yu, F.; et al. Preparation and Application of Decellularized ECM-Based Biological Scaffolds for Articular Cartilage Repair: A Review. *Front. Bioeng. Biotechnol.* **2022**, *10*, 908082. [CrossRef] [PubMed]

17. Neishabouri, A.; Soltani Khaboushan, A.; Daghigh, F.; Kajbafzadeh, A.M.; Majidi Zolbin, M. Decellularization in Tissue Engineering and Regenerative Medicine: Evaluation, Modification, and Application Methods. *Front. Bioeng. Biotechnol.* **2022**, *10*, 805299. [CrossRef] [PubMed]

18. Li, Y.; Xu, Y.; Liu, Y.; Wang, Z.; Chen, W.; Duan, L.; Gu, D. Decellularized Cartilage Matrix Scaffolds with Laser-Machined Micropores for Cartilage Regeneration and Articular Cartilage Repair. *Mater. Sci. Eng. C Mater. Biol. Appl.* **2019**, *105*, 110139. [CrossRef]

19. Gvaramia, D.; Kern, J.; Jakob, Y.; Tritschler, H.; Brenner, R.E.; Breiter, R.; Kzhyshkowska, J.; Rotter, N. Modulation of the Inflammatory Response to Decellularized Collagen Matrix for Cartilage Regeneration. *J. Biomed. Mater. Res. A* **2022**, *110*, 1021–1035. [CrossRef]

20. Guo, W.; Zheng, X.; Zhang, W.; Chen, M.; Wang, Z.; Hao, C.; Huang, J.; Yuan, Z.; Zhang, Y.; Wang, M.; et al. Mesenchymal Stem Cells in Oriented PLGA/ACECM Composite Scaffolds Enhance Structure-Specific Regeneration of Hyaline Cartilage in a Rabbit Model. *Stem Cells Int.* **2018**, *2018*, 6542198. [CrossRef]

21. Liang, J.; Liu, P.; Yang, X.; Liu, L.; Zhang, Y.; Wang, Q.; Zhao, H. Biomaterial-Based Scaffolds in Promotion of Cartilage Regeneration: Recent Advances and Emerging Applications. *J. Orthop. Transl.* **2023**, *41*, 54–62. [CrossRef] [PubMed]

22. Fénelon, M.; Catros, S.; Meyer, C.; Fricain, J.C.; Obert, L.; Auber, F.; Louvrier, A.; Gindraux, F. Applications of Human Amniotic Membrane for Tissue Engineering. *Membranes* **2021**, *11*, 387. [CrossRef]

23. Macečková, Z.; Pergner, J.; Krbec, M.; Urban, M.; Zahradníček, M. Application of Amniotic Membrane in Osteoarthritis Management. *J. Cartil. Jt. Preserv.* **2024**, 100174. [CrossRef]

24. Cao, L.; Tong, Y.; Wang, X.; Zhang, Q.; Qi, Y.; Zhou, C.; Yu, X.; Wu, Y.; Miao, X. Effect of Amniotic Membrane/Collagen-Based Scaffolds on the Chondrogenic Differentiation of Adipose-Derived Stem Cells and Cartilage Repair. *Front. Cell Dev. Biol.* **2021**, *9*, 647166. [CrossRef] [PubMed]

25. Pérez-Silos, V.; Moncada-Saucedo, N.K.; Peña-Martínez, V.; Lara-Arias, J.; Marino-Martínez, I.A.; Camacho, A.; Romero-Díaz, V.J.; Banda, M.L.; García-Ruiz, A.; Soto-Dominguez, A.; et al. A Cellularized Biphasic Implant Based on a Bioactive Silk Fibroin Promotes Integration and Tissue Organization during Osteochondral Defect Repair in a Porcine Model. *Int. J. Mol. Sci.* **2019**, *20*, 5145. [CrossRef]

26. Ballesteros, A.C.V.; Puello, H.R.S.; Lopez-Garcia, J.A.; Bernal-Ballen, A.; Mosquera, D.L.N.; Forero, D.M.M.; Charry, J.S.S.; Bejarano, Y.A.N. Bovine Decellularized Amniotic Membrane: Extracellular Matrix as Scaffold for Mammalian Skin. *Polymers* **2020**, *12*, 590. [CrossRef]

27. Chang, C.H.; Chen, C.C.; Liao, C.H.; Lin, F.H.; Hsu, Y.M.; Fang, H.W. Human Acellular Cartilage Matrix Powders as a Biological Scaffold for Cartilage Tissue Engineering with Synovium-Derived Mesenchymal Stem Cells. *J. Biomed. Mater. Res. A* **2014**, *102*, 2248–2257. [CrossRef]

28. Adamowicz, J.; Pokrywczyńska, M.; Tworkiewicz, J.; Kowalczyk, T.; van Breda, S.V.; Tyloch, D.; Kloskowski, T.; Bodnar, M.; Skopinska-Wisniewska, J.; Marszałek, A.; et al. New Amniotic Membrane Based Biocomposite for Future Application in Reconstructive Urology. *PLoS ONE* **2016**, *11*, e0146012. [CrossRef]

29. Edgar, L.; Altamimi, A.; García Sánchez, M.; Tamburrinia, R.; Asthana, A.; Gazia, C.; Orlando, G. Utility of Extracellular Matrix Powders in Tissue Engineering. *Organogenesis* **2018**, *14*, 172. [CrossRef]

30. Xing, Q.; Qian, Z.; Jia, W.; Ghosh, A.; Tahtinen, M.; Zhao, F. Natural Extracellular Matrix for Cellular and Tissue Biomanufacturing. *ACS Biomater. Sci. Eng.* **2017**, *3*, 1462–1476. [CrossRef]

31. Crapo, P.M.; Gilbert, T.W.; Badylak, S.F. An Overview of Tissue and Whole Organ Decellularization Processes. *Biomaterials* **2011**, *32*, 3233–3243. [CrossRef]

32. Barbulescu, G.I.; Bojin, F.M.; Ordodi, V.L.; Goje, I.D.; Barbulescu, A.S.; Paunescu, V. Decellularized Extracellular Matrix Scaffolds for Cardiovascular Tissue Engineering: Current Techniques and Challenges. *Int. J. Mol. Sci.* **2022**, *23*, 13040. [CrossRef] [PubMed]

33. Chen, D.; Zhang, Y.; Lin, Q.; Chen, D.; Li, X.; Dai, J.; Sun, Y. The Effect of Cartilage Decellularized Extracellular Matrix-Chitosan Compound on Treating Knee Osteoarthritis in Rats. *PeerJ* **2021**, *9*, e12188. [CrossRef] [PubMed]

34. Shin, Y.J.; Shafranek, R.T.; Tsui, J.H.; Walcott, J.; Nelson, A.; Kim, D.H. 3D Bioprinting of Mechanically Tuned Bioinks Derived from Cardiac Decellularized Extracellular Matrix. *Acta Biomater.* **2021**, *119*, 75–88. [CrossRef]

35. Noro, J.; Vilaça-Faria, H.; Reis, R.L.; Pirraco, R.P. Extracellular Matrix-Derived Materials for Tissue Engineering and Regenerative Medicine: A Journey from Isolation to Characterization and Application. *Bioact. Mater.* **2024**, *34*, 494–519. [CrossRef]

36. Kiani, C.; Chen, L.; Wu, Y.J.; Yee, A.J.; Yang, B.B. Structure and Function of Aggrecan. *Cell Res.* **2002**, *12*, 19–32. [CrossRef]

37. Guo, P.; Jiang, N.; Mini, C.; Miklosic, G.; Zhu, S.; Vernengo, A.J.; D'Este, M.; Grad, S.; Alini, M.; Li, Z. Decellularized Extracellular Matrix Particle-Based Biomaterials for Cartilage Repair Applications. *J. Mater. Sci. Technol.* **2023**, *160*, 194–203. [CrossRef]

38. Fernández-Pérez, J.; Ahearne, M. The Impact of Decellularization Methods on Extracellular Matrix Derived Hydrogels. *Sci. Rep.* **2019**, *9*, 14933. [CrossRef]

39. Szwed-Georgiou, A.; Płociński, P.; Kupikowska-Stobba, B.; Urbaniak, M.M.; Rusek-Wala, P.; Szustakiewicz, K.; Piszko, P.; Krupa, A.; Biernat, M.; Gazińska, M.; et al. Bioactive Materials for Bone Regeneration: Biomolecules and Delivery Systems. *ACS Biomater. Sci. Eng.* **2023**, *9*, 5222–5254. [CrossRef]

40. Cramer, M.C.; Badylak, S.F. Extracellular Matrix-Based Biomaterials and Their Influence Upon Cell Behavior. *Ann. Biomed. Eng.* **2020**, *48*, 2132. [CrossRef]

41. Zahiri, S.; Masaeli, E.; Poorazizi, E.; Nasr-Esfahani, M.H. Chondrogenic Response in Presence of Cartilage Extracellular Matrix Nanoparticles. *J. Biomed. Mater. Res. A* **2018**, *106*, 2463–2471. [CrossRef] [PubMed]

42. Gresham, R.C.H.; Bahney, C.S.; Leach, J.K. Growth Factor Delivery Using Extracellular Matrix-Mimicking Substrates for Musculoskeletal Tissue Engineering and Repair. *Bioact. Mater.* **2021**, *6*, 1945. [CrossRef] [PubMed]

43. Zhang, Q.; Lu, H.; Kawazoe, N.; Chen, G. Pore Size Effect of Collagen Scaffolds on Cartilage Regeneration. *Acta Biomater.* **2014**, *10*, 2005–2013. [CrossRef]

44. Dai, C.; Liu, Y. Hepatocyte Growth Factor Antagonizes the Profibrotic Action of TGF-Beta1 in Mesangial Cells by Stabilizing Smad Transcriptional Corepressor TGIF. *J. Am. Soc. Nephrol.* **2004**, *15*, 1402–1412. [CrossRef]

45. Liu, Z.; Zhu, X.; Zhu, T.; Tang, R. Evaluation of a Biocomposite Mesh Modified with Decellularized Amniotic Membrane for Intraperitoneal Onlay Mesh Repair. *ACS Omega* **2020**, *5*, 3550. [CrossRef]

46. Hanai, H.; Jacob, G.; Nakagawa, S.; Tuan, R.S.; Nakamura, N.; Shimomura, K. Potential of Soluble Decellularized Extracellular Matrix for Musculoskeletal Tissue Engineering—Comparison of Various Mesenchymal Tissues. *Front. Cell Dev. Biol.* **2020**, *8*, 581972. [CrossRef] [PubMed]

47. Luo, L.; Eswaramoorthy, R.; Mulhall, K.J.; Kelly, D.J. Decellularization of Porcine Articular Cartilage Explants and Their Subsequent Repopulation with Human Chondroprogenitor Cells. *J. Mech. Behav. Biomed. Mater.* **2016**, *55*, 21–31. [CrossRef]

48. Cheng, N.C.; Estes, B.T.; Young, T.H.; Guilak, F. Genipin-Crosslinked Cartilage-Derived Matrix as a Scaffold for Human Adipose-Derived Stem Cell Chondrogenesis. *Tissue Eng. Part A* **2013**, *19*, 484. [CrossRef]

49. Son, Y.B.; Jeong, Y.I.; Jeong, Y.W.; Hossein, M.S.; Olsson, P.O.; Tinson, A.; Singh, K.K.; Lee, S.Y.; Hwang, W.S. Cell Source-Dependent In Vitro Chondrogenic Differentiation Potential of Mesenchymal Stem Cell Established from Bone Marrow and Synovial Fluid of Camelus Dromedarius. *Animals* **2021**, *11*, 1918. [CrossRef]

50. Lee, J.; Lee, J.Y.; Chae, B.C.; Jang, J.; Lee, E.A.; Son, Y. Fully Dedifferentiated Chondrocytes Expanded in Specific Mesenchymal Stem Cell Growth Medium with FGF2 Obtains Mesenchymal Stem Cell Phenotype In Vitro but Retains Chondrocyte Phenotype In Vivo. *Cell Transpl.* **2017**, *26*, 1673. [CrossRef]

51. Cha, M.H.; Do, S.H.; Park, G.R.; Du, P.; Han, K.C.; Han, D.K.; Park, K. Induction of Re-Differentiation of Passaged Rat Chondrocytes Using a Naturally Obtained Extracellular Matrix Microenvironment. *Tissue Eng. Part A* **2013**, *19*, 978–988. [CrossRef] [PubMed]

52. Youngstrom, D.W.; Cakstina, I.; Jakobsons, E. Cartilage-Derived Extracellular Matrix Extract Promotes Chondrocytic Phenotype in Three-Dimensional Tissue Culture. *Artif. Cells Nanomed. Biotechnol.* **2016**, *44*, 1040–1047. [CrossRef] [PubMed]